Magnetic-Pneumatic Hybrid Soft Actuator

Ito, Kosei
Department of Aeronautics and Astronautics, Kyushu University

Tsumori, Fujio
Department of Aeronautics and Astronautics, Kyushu University

出版情報：Journal of Photopolymer Science and Technology. 36 (3), pp.167-172, 2023-06-15. フォトポリマー学会
バージョン：

Journal of Photopolymer Science and Technology
Volume 36, Number 3 (2023) 167−172 ©2023SPST

Magnetic-Pneumatic Hybrid Soft Actuator

Kosei Ito and Fujio Tsumori*

Department of Aeronautics and Astronautics, Kyushu University,
744 Motooka, Nishi-ku, Fukuoka 819-0395, Japan
**tsumori @aero.kyushu-u.ac.jp*

In this study, we developed a new actuator that can be driven by both magnetic and pneumatic and conducted driving experiments using the fabricated actuator. Soft actuators are widely used as a means of biomimicry. However, many existing actuators that use a single drive source have limited degrees of freedom and deformation capabilities. Recently, hybrid actuators that can be driven by multiple sources have gained attention due to their ability to produce movements that are not achievable by a single drive source. In this study, we fabricated a simple actuator that combines a cylindrical pillar made of silicone material containing magnetic particles with a hollow structure for pneumatic deformation. Three types of actuators with varying diameters and positions of the hollow structure were fabricated, and the drive of each actuator was measured. The pneumatic extensible actuator allows the actuator tip to be manipulated on a fan-shaped two-dimensional plane. The pneumatic bending actuator could manipulate the actuator tip in three dimensions. The actuator with a larger diameter hollow structure could be deformed differently in the same magnetic field by changing the stiffness of the actuator depending on the air pressure. Furthermore, by modifying the hollow structure and the external shape of the actuator, more unique movements can be achieved, and it is expected to be applied to bio-mimicry such as tentacle movement and cilia structure.

Keywords: Soft actuator, Magnetic, Pneumatic, Hybrid actuator, Manipulation, Bio-mimicry

1. Introduction

Soft actuators are made of flexible and lightweight materials, such as silicone rubber, and can be driven by various methods, including pneumatic or hydraulic fluid pressure [1–4], and smart materials that respond to external stimuli like electricity [5,6], magnetic fields [7–28], temperature [29–31], or light [32]. These drive methods enable softer and more delicate movements than conventional rigid actuators that use metal parts, and they are frequently used in biomimicry to replicate human body functions, such as the heart [33] and tongue [34], or natural movements like those of a caterpillar [11,35] or the tentacles of an octopus [36].

Recently, researchers have been developing hybrid-drive soft actuators that combine multiple drive sources, allowing for greater manipulation freedom and larger deformations that are impossible with a single drive source [37,38]. However, the combination of drive sources complicates deformation control and requires a more expensive setup for the drive, limiting their practical applications. To address this issue, we fabricated a simple actuator that can be driven by both a magnetic field and pneumatic pressure by adding a hollow structure for pneumatic deformation to a cylindrical pillar made of silicone material containing magnetic particles.

The driving principles of magnetic field and pneumatic pressure are explained as follows. To drive an actuator using a magnetic field, the actuator containing magnetic particles is magnetized, which is a process of applying a strong magnetic field to the particles to leave residual magnetization. When an external magnetic field is applied to a magnetized actuator, the magnetic moment acts in the direction of the external magnetic field and the direction of the remanent magnetization, causing the actuator to deform (Fig. 1). Pneumatic actuation deforms the

Received April 5, 2023
Accepted May 18, 2023

actuator by increasing the internal pressure like a balloon. In the cylindrical balloon fabricated in this study, pneumatic deformation causes elongation when the film thickness is uniform and bending when the film thickness is anisotropic (Fig. 2). A drive was also developed to change the stiffness of the actuator by depressurizing it and concaving its cross-section.

In this study, we fabricated three types of actuators: one that undergoes elongation deformation when the hollow structure is pressurized, one that undergoes bending deformation when pressurized, and one whose stiffness is changed by depressurization. Driving experiments were conducted using these actuators in combination with magnetic field driving, and the resulting deformation was measured to investigate the driving characteristics.

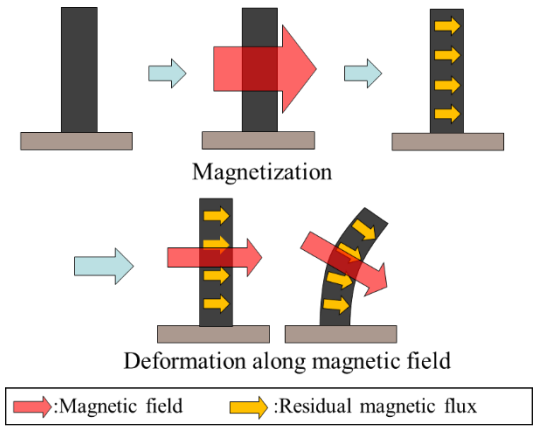

Fig. 1. Schematic illustration of a magnetically driven soft actuator.

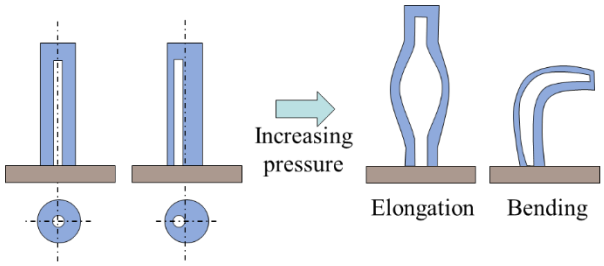

Fig. 2. Schematic illustration of a pneumatic driven soft actuator with a central and eccentric hollow cavity.

2. Materials and driving system

2.1. Materials

This section provides information about the materials and methods used to fabricate the magnetic field/pneumatic hybrid actuator. The Ecoflex 00-30 (Smooth-On) was chosen as the two-component silicone resin material due to its high flexibility and durability. SF-500 (DOWA F-Tec), with an average particle diameter of 1.42 μm, was selected as the magnetic particle for the actuator. Strontium ferrite was used to make the particles, which is a hard-magnetic material commonly used as a permanent magnet material.

To make the actuator, a mold was created by combining three parts: a plastic tube with an inner diameter of 4.0 mm and a length of 20 mm, a metal pin with a diameter of 0.80 mm and a length of 22 mm, and a part to fix the metal pin. The fixed parts were made of PLA (Poly-Lactic Acid) resin using a 3D printer (Original Prusa i3 Mk3, Prusa Research). For the actuator used in section 3.3, which deforms the cross-section by depressurizing, a thick metal pin with a diameter of 2 mm was used.

2.2. Fabrication

The fabrication process for the actuator is presented in Fig. 3. Firstly, magnetic particles (20 mass%) were added to silicone rubber. The mixture was then stirred and deaerated using a stirring and deaeration device (Kakuhunter, Shasin Kagaku CO., LTD.) to achieve a uniform dispersion of the magnetic particles, resulting in the production of magnetic elastomer. The magnetic particle-dispersed elastomer was then injected into a mold using a syringe, and a fixing component was inserted to secure the position of a metal pin at the top. The sample was then placed in a vacuum chamber for 1.2 ks (20 min) to remove air bubbles. The silicone was cured at 50 °C for 3.6 ks (1 h). The fixing component at the top was then removed, and the cured sample was slid up slightly while still attached to the metal pin. Additional magnetic particle-dispersed elastomer was injected from the top, and the top hole was closed by placing the sample in a vacuum chamber for 600 s (10 min) to fill it with silicone. The silicone was then cured at 50 °C for 1.8 ks (30 min). Finally, the sample was removed from the mold and connected to an air supply connector (Mini Tube Connector, ARAM Corporation) for inflation. The gaps at the connection were filled with instant adhesive (CA-522, CEMEDINE CO., LTD.).

2.3. Driving System

A system was constructed to enable the application of both magnetic field and pneumatic pressure concurrently. To generate a uniform parallel magnetic field of 50 mT at the center of the system, permanent magnets were placed diagonally as illustrated in Fig. 4. Air pressure was regulated by a syringe that was connected to the actuator from underneath the stage.

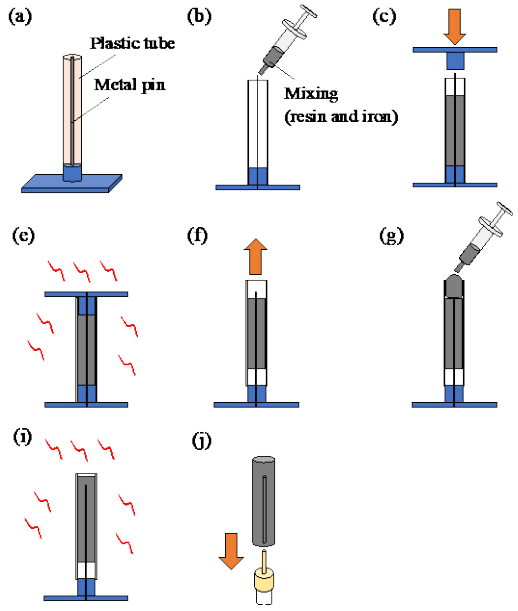

Fig. 3. Fabrication process for actuators that can be driven by both magnetic and pneumatic fields.

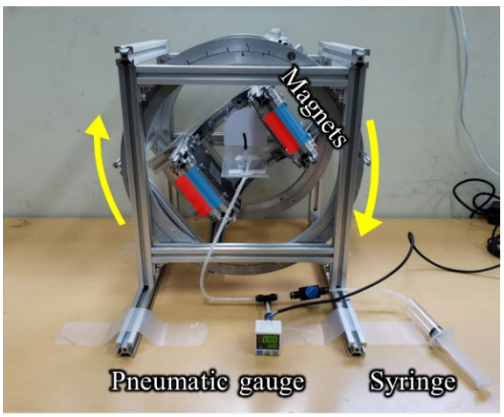

Fig. 4. Systems for magnetic and pneumatic drive.

3. Experimental

3.1. Pneumatic extension actuator

Snapshots (a) and measured displacements of a pneumatic extension actuator (b) are shown in Fig. 5. The internal pressure was fixed at 0, 10, 25, and 30 kPa, the angle of the parallel magnetic field was rotated between 0 and 360 degrees, and displacements were measured every 30 degrees.

The magnetic field drive only allows movement on a circular arc, while the pneumatic drive only allows deformation by extending and retracting in the longitudinal direction. By combining magnetic and pneumatic drive, we were able to extend the operation range to a two-dimensional plane.

The actuator is tilted to the left (negative side of the x-axis) as a whole, which is because the actuator could not be fixed in a strictly symmetrical manner or due to a fabrication error. In addition, when 30 kPa was applied, the actuator was greatly extended, which may have caused it to fall outside the range of the uniform parallel magnetic field of the device. To accurately apply a uniform parallel magnetic field even after stretching under pressure, the actuator must be made smaller.

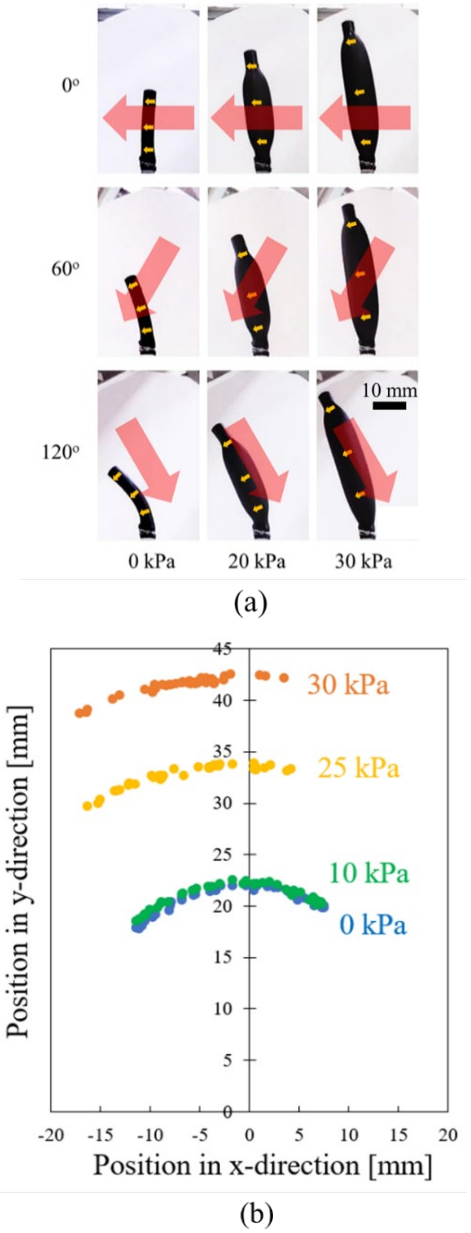

Fig. 5. Snapshots and measured displacements of a pneumatic extension actuator.

3.2. Pneumatic bending actuator

We fabricated an actuator that bends when pressurized by displacing the center of the hollow structure by 0.5 mm from the axis. When this actuator is pressurized, it deforms as shown in Fig. 6(a). The top line in Fig.6(a) shows the side view, and the following lines show the front view. This actuator begins to expand at 15 kPa and

subsequently expands by the amount of air injected without any change in air pressure. Thus, we divided the expanding phase into three stages labeled as (1), (2), and (3) at 15 kPa. Magnetization was applied perpendicular to the direction in which pneumatic pressure causes bend deformation. The actuator was set to bend in the z-axis direction, fixed at 0 kPa and three stages of expansion at 15 kPa, and driven by the application of a magnetic field.

Figure 6(b) show snapshots taken from the front and a plot of the actuator tip, respectively. The actuator was bent in the forward direction by the pneumatic drive, and then the tip was deformed in a circular motion by the magnetic drive. The pneumatic bending actuator, in combination with the magnetic field, was able to manipulate the actuator tip in three dimensions.

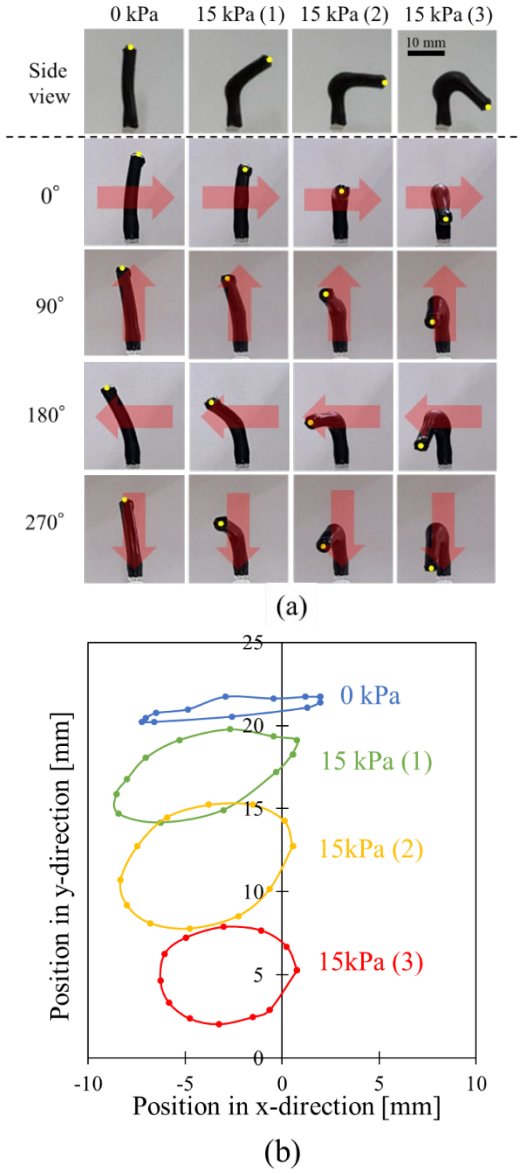

Fig. 6. Snapshots and measured displacements of a pneumatic bending actuator. The top line of (a) shows the side view, and the following lines show the front view.

3.3. Stiffness change actuator

We developed an actuator with a larger hollow diameter compared to the ones used in sections 3.1 and 3.2, which utilizes deformation of the cross section induced by depressurization. The internal pressure was set at -20, 0, and 8 kPa, and the angle of the parallel magnetic field was rotated between 0 and 360 degrees, with the displacement being measured every 10 degrees. During depressurization, the actuator was externally pressed on the side to assist the cross-section in bending concavely in the desired direction.

Figure 7 displays a snapshot of the actuator and the measured tip displacement. By collapsing the hollow portion of the actuator under reduced

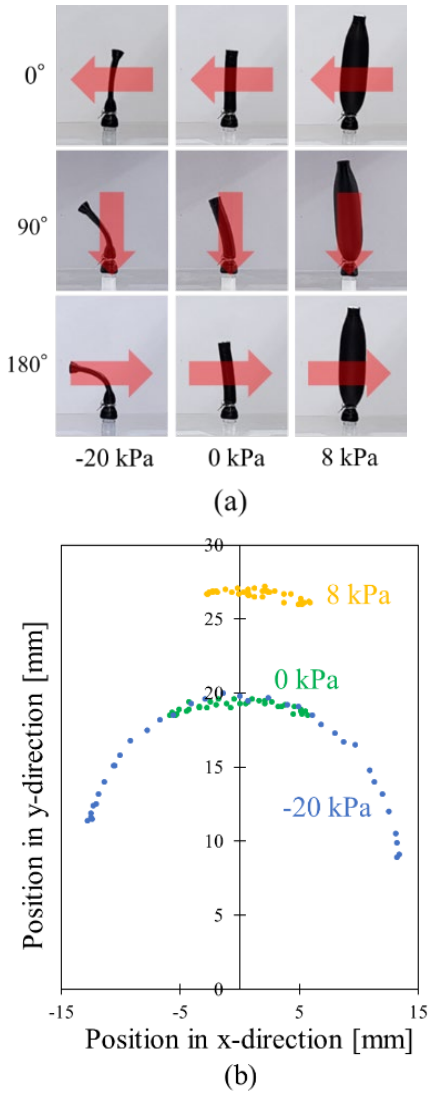

Fig. 7. Snapshots and measured displacements of an actuator using stiffness change actuator.

pressure, the moment of inertia of area was reduced, increasing the deformation caused by the magnetic field. The actuator could also be elongated when pressurized.

4. Conclusion

We have developed an actuator that is capable of being powered by both air pressure and a magnetic field. By altering the diameter and location of the hollow structure, we have produced three distinct types of actuators. The pneumatic extensional actuator can be manipulated in a fan-shaped two-dimensional plane, while the pneumatic bending actuator can be driven in a circular motion in addition to the forward bending. The actuator with a larger hollow structure was able to achieve unique deformations by adjusting the stiffness through negative pressure. Our actuator design has the potential to be further developed for biomimetic applications, such as mimicking the movements of biological tentacles and cilia structures.

Acknowledgements

This work was supported by MEXT KAKENHI Grant Numbers JP22H05685 and JP23H04319.

References

1. R. F. Shepherd, F. Ilievski, W. Choi, S. A. Morin, A. A. Stokes, A. D. Mazzeo, X. Chen, M. Wang, and G. M. Whitesides, *Proc. Natl. Acad. Sci. U S A,* **108** (2011) 20400.
2. P. Ohta, L. Valle, J. King, K. Low, J. Yi, C. G. Atkeson, and Y. L. Park, *Soft Robotics*, **5** (2018) 204.
3. Y. S. Narang, J. J. Vlassak, and R. D. Howe, *Adv. Funct. Mater.*, **28** (2018) 1707136.
4. K. Becker, C. Teeple, N. Charles, Y. Jung, D. Baum, J. C. Weaver, L. Mahadevan, and R. Wood, *Proc. Natl. Acad. Sci. U S A* ,**119** (2022) e2209819119.
5. R. Kornbluh, R. Pelrine, J. Eckerle, and J. Joseph, *Proc. IEEE ICRA*, **3** (1998) 2147.
6. J. Bernat and J. Kołota, *Energies*, **14** (2021) 5633.
7. H. Shinoda and F. Tsumori, *Proc. IEEE-MEMS*, (2020) 497.
8. F. Tsumori and J. Brunne, *Proc. IEEE-MEMS*, (2011) 1245.
9. T. Murakami and F. Tsumori, *Jpn. J. Appl. Phys.*, **61** (2022) SD1014.
10. H. Shinoda and F. Tsumori, *Jpn. J. Appl. Phys.*, **57** (2018) 06HJ05.
11. K. Maeda, H. Shinoda, and F. Tsumori, *Jpn. J. Appl. Phys.*, **59** (2020) SIIL04.
12. H. Shinoda, S. Azukizawa, K. Maeda, and F. Tsumori, *J. Electrochem. Soc.*, **166** (2019) B3235.
13. S. Azukizawa, H. Shinoda, K. Tokumaru, and F. Tsumori, *J. Photopolym. Sci. Technol.*, **31** (2018) 139.
14. F. Tsumori, A. Saijou, T. Osada, and H. Miura, *Jpn. J. Appl. Phys.*, **54** (2015) 06FP12.
15. M. Furusawa, K. Maeda, S. Azukizawa, H. Shinoda, and F. Tsumori, *J. Photopolym. Sci. Technol.*, **32** (2019) 309.
16. R. Marume, F. Tsumori, K. Kudo, T. Osada, and K. Shinagawa, *Jpn. J. Appl. Phys.,* **56** (2017) 06GN15.
17. S. Azukizawa, F. Tsumori, H. Shinoda, K. Tokumaru, K. Kudo, and K. Shinagawa, *Proc. MicroTAS*, (2020) 623.
18. F. Tsumori, R. Marume, A. Saijou, K. Kudo, T. Osada, and H. Miura, *Jpn. J. Appl. Phys.*, **55** (2016) 06GP19.
19. F. Tsumori and K. Tokumaru, *Proc. MicroTAS*, (2020) 396.
20. S. Shigetomi and F. Tsumori, *J. Photopolym. Sci. Technol.*, **34** (2021) 375.
21. S. Gaysornkaew and F. Tsumori, *Jpn. J. Appl. Phys.*, **60** (2021) SCCL02.
22. H. Shinoda, S. Azukizawa, and F. Tsumori, in *22nd International Conference on Miniaturized Systems for Chemistry and Life Sciences, MicroTAS 2018*, (2018) 679.
23. S. Shigetomi, H. Takahashi, and F. Tsumori, *J. Photopolym. Sci. Technol.*, **33** (2020) 193.
24. K. Ninomiya, S. Gaysornkaew, and F. Tsumori, *Proc. IEEE-MEMS*,(2022) 235.
25. S. Gaysornkaew, D. V. Vargas, and F. Tsumori, *IEEE CYBCONF*,(2021) 061.
26. H. Shinoda, S. Azukizawa, K. Maeda, and F. Tsumori, *ECS Trans.*, **88** (2018) 89.
27. F. Tsumori, H. Kawanishi, K. Kudo, T. Osada, and H. Miura, *Jpn. J. Appl. Phys.*, **55** (2016) 06GP18.
28. F. Tsumori, N. Miyano, A. Fukui, K. Sagawa, and H. Kotera, *Proc. COMPLAS*, (2007) 354.
29. K. Takashima, J. Rossiter, and T. Mukai, Sens. actuators. A Phys., **164** (2010) 116.
30. A. Miriyev, K. Stack, and H. Lipson, *Nat. Commun.*, **8** (2017) 596.
31. T. Noguchi and F. Tsumori, *Jpn. J. Appl. Phys.*, **59** (2020) SIIL08.
32. M. Pilz da Cunha, S. Ambergen, M. G. Debije, E. F. G. A. Homburg, J. M. J. den Toonder, and A. P. H. J. Schenning, *Adv. Sci.*, **7** (2020) 1902842.

33. E. T. Roche, M. A. Horvath, I. Wamala, A. Alazmani, S. E. Song, W. Whyte, Z. Machaidze, C. J. Payne, J. C. Weaver, G. Fishbein, J. Kuebler, N. v. Vasilyev, D. J. Mooney, F. A. Pigula, and C. J. Walsh, *Sci. Transl. Med.*, **9** (2017) eaaf3925.
34. N. Endo, Y. Kizaki, and N. Kamamichi, *J. Robot. Mechatron*., **32** (2020) 894.
35. P. Karipoth, A. Christou, A. Pullanchiyodan, and R. Dahiya, *Adv. Intell. Syst*., **4** (2022) 2100092.
36. B. Mazzolai, A. Mondini, F. Tramacere, G. Riccomi, A. Sadeghi, G. Giordano, E. del Dottore, M. Scaccia, M. Zampato, and S. Carminati, *Adv. Intell. Syst*., **1** (2019) 1900041.
37. J. E. Lee, Y. Sun, Y.-C. Sun, I. R. Manchester, and H. E. Naguib, *Appl. Mater. Today*, **29** (2022) 101681.
38. B. Han, Z. C. Ma, Y. L. Zhang, L. Zhu, H. Fan, B. Bai, Q. D. Chen, G. Z. Yang, and H. B. Sun, *Adv. Funct. Mater.*, **32** (2022) 2110997 .